A novel protein–mineral interface

Dmitriy Alexeev[1], Haizhong Zhu[2], Maolin Guo[2,3], Weiqing Zhong[2,4], Dominic J.B. Hunter[2], Weiping Yang[2,4], Dominic J. Campopiano[2] and Peter J. Sadler[2]

Published online 24 February 2003; corrected 10 March 2003 (details online); doi:10.1038/nsb903

Transferrins transport Fe^{3+} and other metal ions in mononuclear-binding sites. We present the first evidence that a member of the transferrin superfamily is able to recognize multi-nuclear oxo-metal clusters, small mineral fragments that are the most abundant forms of many metals in the environment. We show that the ferric ion–binding protein from *Neisseria gonorrhoeae* (nFbp) readily binds clusters of Fe^{3+}, Ti^{4+}, Zr^{4+} or Hf^{4+} in solution. The 1.7 Å resolution crystal structure of Hf–nFbp reveals three distinct types of clusters in an open, positively charged cleft between two hinged protein domains. A di-tyrosyl cluster nucleation motif (Tyr195-Tyr196) is situated at the bottom of this cleft and binds either a trinuclear oxo-Hf cluster, which is capped by phosphate, or a pentanuclear cluster, which in turn can be capped with phosphate. This first high-resolution structure of a protein–mineral interface suggests a novel metal-uptake mechanism and provides a model for protein-mediated mineralization/dissimilation, which plays a critical role in geochemical processes.

Organisms have developed sophisticated mechanisms for the uptake of Fe^{3+} and other metal ions from the environment. Metals in mineral form are used as sources of energy by geobacteria[1], which are critical in the control of mineral growth and phase transformations[2]. The recognition of minerals by microbial proteins is of current interest because microbes can affect the chemistry and distribution of nearly all elements in the periodic table[3,4]. Little structural information is currently available about the interactions between proteins and metal clusters during the initial stages of protein-mediated mineralization and mineral acquisition by bacteria. Here we report the surprising discovery that an iron-binding protein in the transferrin superfamily can recognize a variety of metal clusters in its iron-binding cleft, a finding that has potential implications for our understanding of metal uptake mechanisms.

Many pathogenic microorganisms require iron for virulence[5]. However, iron acquisition is a major problem for them in aerobic environments because aquated Fe^{3+} ions are highly acidic and readily form hydroxide- and oxide-bridged polymers and insoluble FeO(OH) (rust) at neutral or alkaline pH[6]. Therefore, pathogenic Gram-negative bacteria, such as *Neisseria gonorrhoeae*, *Neisseria meningitidis* and *Haemophilus influenzae*, synthesize the iron-binding protein Fbp to capture iron presented at the outer membrane and transport it across the periplasm. Fbp, a single polypeptide chain of 309 amino acids, shows the same polypeptide topology as the two lobes of serum transferrin and lactoferrin despite a lack of significant sequence similarity[7,8]. The Fe^{3+}-binding site is in an interdomain cleft — a 'Venus fly-trap' — that is open in the apo protein and closed when Fe^{3+} is bound. Fbp has been reported to bind one Fe^{3+} strongly but reversibly[9], as does each lobe of transferrin[10]. We sought to determine whether other metals bind strongly to Fbp from *N. gonorrhoeae* (nFbp) as a possible basis for the design of novel metalloantibiotics.

Multinuclear metal binding

The group four metal ions Ti^{4+}, Zr^{4+} and Hf^{4+}, similar to Fe^{3+}, are highly acidic and, therefore, expected to bind strongly to transferrin[11]. They have a high affinity for oxygen ligands — for example, hydroxide, oxide, phosphate and phenolate — and can be found along with Fe^{3+} in the same geological minerals[12]. Ti^{4+} has antibacterial properties[13] and binds strongly to human transferrin[14]. There is interest in the binding of Hf^{4+} to transferrin because of its chemical similarity to Pu^{4+}; injected Hf^{4+} is almost totally bound to transferrin in animal serum[15].

The molar ratio of protein:Fe:phosphate (P) in isolated recombinant holo-nFbp overexpressed in the *Escherichia coli* periplasm is 1:1:1 (Table 1). Addition of an equimolar amount of Hf^{4+} (as the mononuclear complex $[Hf(NTA)_2]^{2-}$) to holo-nFbp led to displacement of 47% of the bound Fe (monitored by the intensity decrease of the tyrosinate-to-Fe^{3+} charge-transfer band at 481 nm in 100 mM NaCl, 4 mM phosphate and 25 mM $NaHCO_3$, pH 7.4, at 310 K). To fully load nFbp with Hf, apo nFbp was reacted with a 50-fold molar excess of the mononuclear chelated Hf^{4+} complex. Unexpectedly, the Hf–nFbp product contained 4.0 Hf and 1.4 P per mol protein (Table 1). The presence of bound phosphate was confirmed by ^{31}P-NMR spectroscopy (new peaks shifted downfield from free phosphate by 2–3 p.p.m.; data not shown). Other metal ions, including Fe^{3+} itself, yielded similar binding patterns. Treatment of apo nFbp with excess chelated Fe^{3+} in the presence of phosphate gave rise to 2–3 mol Fe per mol protein (Table 1). Attempts to remove the excess bound Fe^{3+} by treatment with phosphate ($FePO_4$ is insoluble) did not restore the 1:1 Fe:P ratio (Table 1). Treatment of native mono-ferric holo-nFbp with a large excess of chelated Fe^{3+} did not lead to additional binding of Fe, although the bound phosphate was readily removed. The pathway for multinuclear loading, therefore, does not seem to involve the mononuclear form of the protein[7], which is isolated from bacteria.

Conformational heterogeneity in crystals

We crystallized and solved the three-dimensional structure of Hf–nFbp, containing 4.8 Hf^{4+} per mol protein, at 1.7 Å resolution by molecular replacement (Table 2). Hemihedral twinning

[1]Institute of Cell and Molecular Biology, Michael Swann Building, University of Edinburgh, Mayfield Road, Edinburgh EH9 3JR, U.K. [2]School of Chemistry, University of Edinburgh, West Mains Road, Edinburgh EH9 3JJ, UK. [3]Current address: Department of Molecular Biology and Biochemistry, University of California, Irvine, California 92697, USA. [4]Current address: School of Pharmacy, Second Military Medicine University, Shanghai 200433, China.

Correspondence should be addressed to P.J.S. *e-mail: P.J.Sadler@ed.ac.uk*

Table 1 Analysis of nFbp samples

Sample	Treatment[1]	Mol element per mol protein		
		Fe	P	Other
Holo-native	As isolated[2]	1.04 ± 0.03	0.98 ± 0.04	
Apo/Fe	50 × $[Fe(NTA)_2]^{3-}$; 10 mM Tris, pH 7.8, 12 h	2.4 ± 0.2	0.05 ± 0.08	
Apo/Fe/P_i[3]	10 × $[Fe(NTA)_2]^{3-}$; 10 mM Tris, pH 7.8, then 10× phosphate, 1.5 h	1.8 ± 0.1	1.1 ± 0.1	
Holo/Fe	10 × $[Fe(NTA)_2]^{3-}$; 10 mM Tris, pH 8.0, 4 h	1.10 ± 0.03	0.20 ± 0.01	
Apo/Ti[4]	100 × $[Cp_2TiCl_2]$ (in 10% DMSO, 100 mM NaCl); 10 mM Tris, pH 8.0, 5 h	–	–	Ti 3.4 ± 0.1
Apo/Zr[5]	6 × $[Zr(NTA)_2]^{2-}$; 10 mM HEPES, pH 7.4, 10 mM phosphate, 10 mM HCO_3^-, 24 h	0.07 ± 0.01	1.10 ± 0.10	Zr 3.65 ± 0.40
Apo/Hf	50 × $[Hf(NTA)_2]^{2-}$; 100 mM NaCl, 4 mM phosphate, 25 mM HCO_3^-, pH 7.4, 3 h	–	1.39 ± 0.04	Hf 4.03 ± 0.10

[1]Representative experiments listed. Molar excess (for example, 10×) is relative to protein concentration. Cluster binding was found over a wide range of conditions (salt concentrations, buffers, pH). Apo Fbp was incubated with metal ions at 310 K, and the unbound metal was removed by gel filtration (for example, PD-10 column) and/or by ultrafiltration. NTA = nitrilotriacetate.
[2]Extensive washing with 10 mM Tris-HCl, pH 7.8, led to loss of phosphate (Fe = 1.10 ± 0.02 and P = 0.1 ± 0.03).
[3]Tyr → Fe^{3+} charge-transfer band shifted from 481 nm for native holo-nFbp to 464 nm.
[4]Ti^{4+} loading gives a tyrosinate-to-Ti^{4+} charge-transfer band at 323 nm (similar to Ti^{4+} human serum transferrin)[40]. Cp = cyclopentadienyl.
[5]Crystalline mononuclear $K_2[Zr(NTA)_2]•2H_2O$ was used.

and the complex arrangement of nine protein molecules (labeled A–I) in the asymmetric unit (space group $P3_2$, Fig. 1) presented severe problems (see Methods) but the structure was finally solved to R_{cryst} = 16.5% and R_{free} = 26.4%.

The well-known fold of Fbp comprises two hinged α/β domains. A single Fe^{3+} ion is octahedrally coordinated to His9 and Glu57 from the N-terminal domain, di-tyrosyl Tyr195-Tyr196 from the hinge area, a water molecule and phosphate as an obligatory synergistic anion bound to the C-terminal domain[7,8]. In the apo protein, the domains are open and mono-Fe^{3+} binding is accompanied by a hinge closure of ~26°. We found a variety of Hf^{4+} ion clusters bound in the metal-binding pocket. However, the interdomain hinge remained open and the side chains of His9 and Glu57, previously identified as Fe^{3+} ligands in closed mono-Fe–nFbp, are swung away from the metal-binding site.

The hinge angles of the nine molecules in the crystal vary. They are distinctively wider for the group of three molecules G, H and I by 5.6° on average, with the maximum difference of 8.4° between molecules D and H. The crystal environment of the metal-binding pocket for this group is also distinct (Fig. 1), as is the structure of the metal cluster (described below). The observed structural diversity of the Hf^{4+} clusters seems to be linked to variations in the protein conformation and in the crystal environment.

Unexpectedly for cation binding, the surface of the Hf^{4+}-binding pocket is positively charged (blue, Fig. 2) and its nearest crystal contact is also basic for all nine molecules (Fig. 1). Hf^{4+}

a

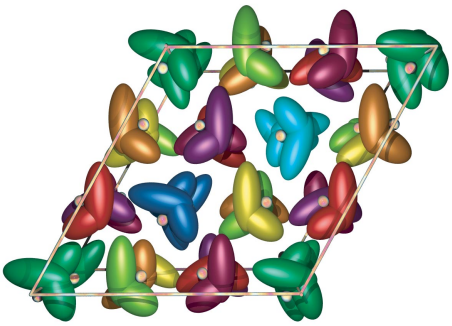

b

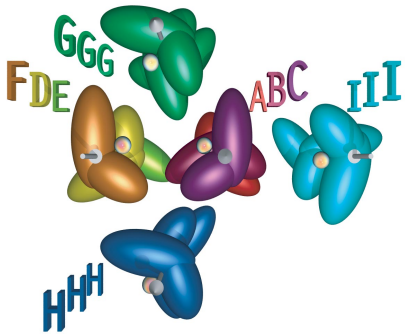

c

C↑↑G Arg22	**F**↓↑G Lys244	**G**↑↑C Arg48
B↑↑H Arg22	**D**↓↓I Arg22	**H**↑↑B Arg48
A↑↓I Lys244	**E**↓↑H Lys244	**I**↓↓D Arg48

Fig. 1 Arrangement of molecules A–I in the unit cell of Hf-nFbp. All nine molecules are individually colored (together with their crystallographically identical copies). The two hinged domains of each protein molecule are represented by intersecting ellipsoids (the N-terminal domain is bigger). Small metallic balls in the middle indicate metal clusters. ***a***, The complete unit cell (space group $P3_2$, with the *z*-axis pointing towards the viewer). ***b***, Stacks of the nine protein molecules A–I in the asymmetric unit along the *z*-axis. Each of the stacks G, H and I lies on a crystallographic three-fold screw axis (not shown), which is therefore made of identical molecules. All identical molecules G have the same color, as do molecules H and I. The directions of arrows running through the hinge area of the protein indicate different orientations of the stacks along the *z*-axis (down for I, up for G and H). The stack ABC (arrow up) is antiparallel to the stack FDE (arrow down). Both ABC and FDE are made of similar, but not identical, molecules, which are therefore differently colored. Individual molecules in these stacks are related by approximate noncrystallographic three-fold screw symmetry and have slightly different conformations. POV-Ray (*http://www.povray.org/*) was used to generate (*a*,*b*). ***c***, Crystal contacts of the metal clusters of molecules **A–I** (bold letters) with their nearest neighbors in the unit cell (plain letters) and the mutual orientation of these nearest-neighbor proteins (parallel or antiparallel). All metal clusters face a positively charged amino acid (Arg or Lys). The entry '**C**↑↑G Arg22' indicates that the metal cluster of molecule C (from the stack ABC) faces Arg22 of molecule G from the parallel stack G. The crystal contacts fall into three general categories: the clusters of the molecules GHI face an Arg48 from a parallel stack (as indicated by ↑↑ or ↓↓), the clusters of BCD face Arg22 from a parallel stack as well, and the clusters of AEF face Lys244 in the antiparallel orientation (↑↓or ↓↑).

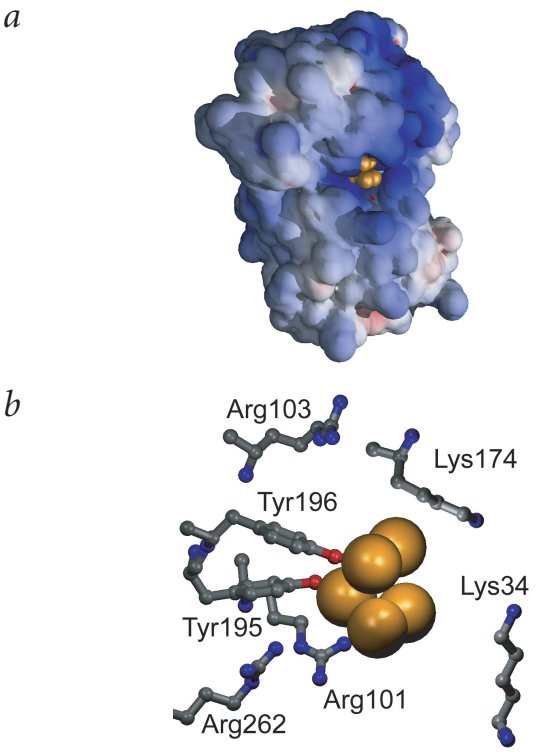

Fig. 2 Metal nanocluster in the positively charged protein-binding pocket of molecule G. ***a***, The positively charged molecular surface around the metal pocket (calculated by GRASP[37]), as indicated in blue. ***b***, Lys and Arg residues in the vicinity of the Hf ions (gold spheres) in the cluster binding pocket. Bridging oxygens and the phosphate are omitted for clarity (Fig. 3*d* for these details). Arg101 is completely conserved in all Fbp sequences.

ions are not in direct contact with any of the protein atoms, except for the phenolate oxygens of Tyr195 and Tyr196, to which they are bonded. Negatively charged oxygen atoms shield Hf^{4+} ions and bridge them in a manner similar to the structure of the mineral HfO_2[16] (Fig. 3). Clusters in the protein mirror the structural heterogeneity of the mineral, which can adopt a variety of crystal forms, usually with coordination numbers of six, seven or eight. These observations suggest that Fbp might be able to acquire mineral oxo-metal clusters *in vivo*.

Trinuclear cluster

The cleft of molecule D is the most closed and contains the smallest cluster of only three metals — Hf1, Hf2 and Hf3 (electron density, Fig. 3*a*). Trinuclear cores of Hf^{4+} ions are common in inorganic complexes containing alkoxide, aryloxide, hydroxide and oxide ligands[17,18]. All three metal atoms are well ordered in the crystal. Hf1 is coordinated to Tyr196, Hf2 to Tyr195, and Hf3 to Hf1 and Hf2 through the bridging oxygens (Fig. 3*b*). This trinuclear cluster is capped by a phosphate, which faces outward from the binding pocket. Each metal has pentagonal bipyramidal coordination to seven oxygens. The five equatorial oxygens are oxides (or hydroxides), and the axial oxygens are from tyrosinate (or water for Hf3) and phosphate. The Hf···Hf distances range from 3.6 to 3.8 Å, and the Hf···O distances from 1.9 to 3.0 Å, with the Hf-tyrosinate bonds being the shortest. The Tyr195-Tyr196 O···O distances of 4.03–4.48 Å are significantly longer than in holo-Fe–nFbp (3.01 Å)[7], where both tyrosines are bound to a single Fe^{3+}. The overall calculated charge on the first coordination shell is –7 (if all four bridging oxygens are oxide). The net positive surface charge on the metal-binding cleft (Fig. 2) may facilitate formation of the protein-cluster complex. An example of this is the assembly of the molybdenum-iron (MoFe) protein of nitrogenase, which involves insertion of a negatively charged MoFe cofactor cluster into a positively charged funnel in the apo protein[19].

Pentanuclear clusters

All molecules in the group A–F, except D, contain similar clusters of five Hf^{4+} ions. In these, the bound phosphate present in the trinuclear cluster (Fig. 3*b*) is replaced by an oxo-metal ion (Hf4, Fig. 3*c*). As in cluster D, the Hf1, Hf2 and Hf3 ions are fully ordered. The additional two ions Hf4 and Hf5 point into the solvent and are disordered. High electron density peaks (>10 σ) and strong anomalous signals (>3 σ) confirm that they are Hf ions, and their high temperature factors (*B*-factor = 95 $Å^2$) indicate that they are mobile. Hf5 forms an oxygen-bridged triangle with Hf1 and Hf4, similar to the triangle Hf1–Hf2–Hf3 of cluster D but without the central oxygen. Both Hf4 and Hf5 are octahedrally coordinated to six oxygens.

Molecules A–C have similar hinge angles and crystal contacts (Fig. 1) and contain similar metal clusters. The clusters of the molecules E and F differ from the clusters in A–C by an even higher mobility/disorder of Hf5. The clusters G–I are similar and contain five metal ions and an additional phosphate (Fig. 3*d*). Unlike cluster D, the phosphate bridges Hf1 to Hf4 and Hf5, which are mobile in A, B, C, E and F. The phosphate-bound ions Hf4 and HF5 become well ordered (*B*-factor = 42 $Å^2$) in the group G–I. The other pair of ions, Hf2 and Hf3, which is well ordered in A–F, becomes mobile (*B*-factor = 92 $Å^2$) in G–I, although Hf2 is bonded to Tyr195 and Hf3 is the most buried in the binding pocket. The phosphate-capped ordered cluster Hf1–Hf4–Hf5 is identical to that of Hf1–Hf2–Hf3 in D, but situated further away from the bottom of the metal binding pocket. Positional disorder seems to be associated with phosphate binding and not with the tyrosyl ligands. The size of the clusters correlates with the hinge-angle opening: the most closed molecule D contains the smallest cluster and the larger clusters are found in the more open molecules G–I.

Clusters in mammalian transferrin?

Hf–nFbp is the first observation of multinuclear binding to the open form of Fbp. Open transferrin conformations are known with a single bound Fe^{3+} ion[20–22]. Domain closure was not observed for mammalian transferrin treated with Hf(NTA) in solution[23]. When we treated human serum apo transferrin with a 30-fold molar excess of $[Hf(NTA)_2]^{2-}$ under similar conditions as those used for Hf–nFbp preparations, we found a bound Hf:protein:phosphate ratio of 3.5:1:1.1 (data not shown), similar to Fbp. This suggests that at least the N-lobe, which is wide open in the apo protein, binds a Hf cluster. The C-lobe may not be able to open wide enough to bind metal clusters, and this may be relevant to the functional difference between the two lobes.

Cluster binding seems to be more facile than mononuclear binding, which requires a conformational transition plus a synergistic helper anion (phosphate or carbonate). Helper anions are redundant for cluster binding: oxygens of the oxo clusters take the place of the synergistic anion in the positively charged binding site. The cleft of the N-lobe of transferrin can open some 20° wider[24] than Fbp and can contain more phosphate-binding sites[22], potential anchors for oxo-metal clusters. This, together with the high affinity of Fbp for multimetal clusters, suggests that the N-lobe of transferrins could also bind metal clusters.

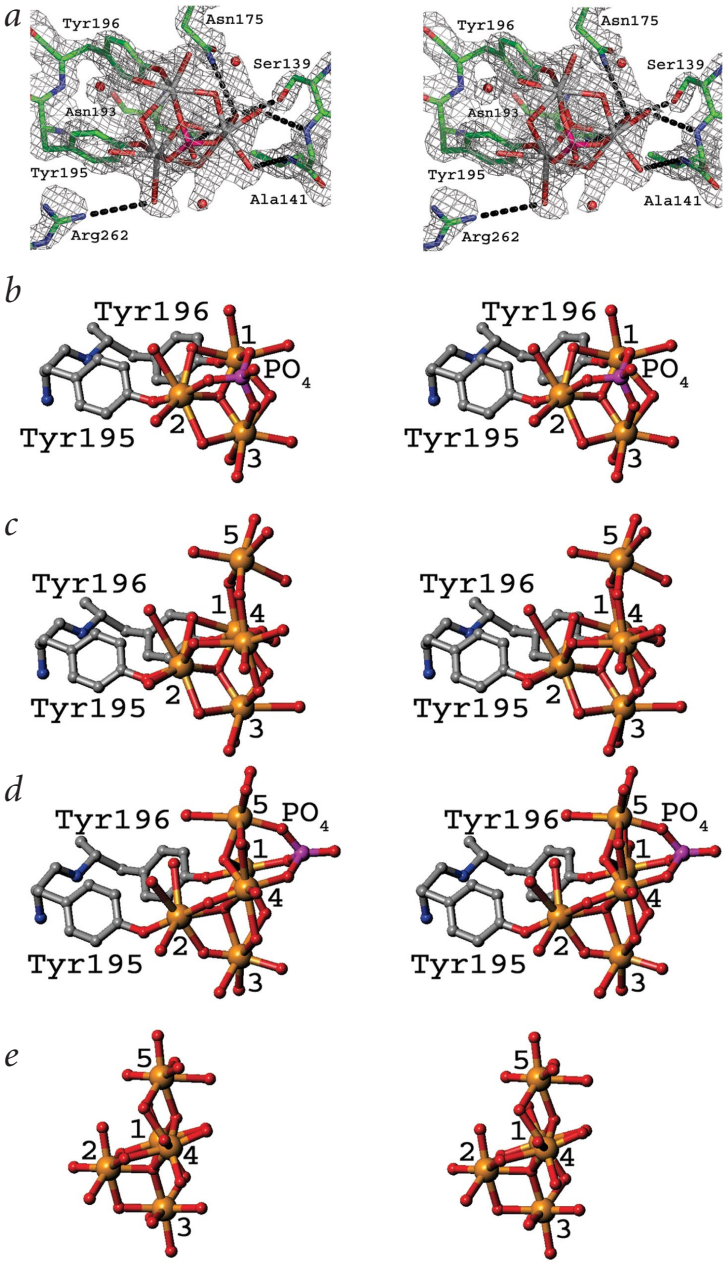

Fig. 3 Stereo views of Hf coordination in the protein nanoclusters and the mineral HfO_2. The numbering of the ions Hf1–Hf5 corresponds to the strength order of the electron density peaks in the molecules A–F. Hf1 (bound to Tyr196) is the most ordered in all clusters. ***a***, SigmaA[38]-weighted ($2F_o - F_c$) electron density map for the smallest cluster (D) calculated with CNS[34] using the phases from the final model refined for crystal 2; contouring is at 1.5 σ. The small, unconnected red balls represent water molecules. The metal ions are coordinated to the protein through the phenolate oxygens of Tyr195 and Tyr196. ***b***, The smallest cluster in molecule D. Hf^{4+} ions are gold; and oxygens, red. Phosphate caps the Hf1, Hf2 and Hf3 ions. ***c***, The metal cluster in molecule A (clusters in B, C, E and F are similar). This cluster contains five Hf ions and no bound phosphate. ***d***, Cluster in molecule G (as in Fig. 2). The ions Hf1, Hf4 and Hf5 are capped by phosphate. The clusters in H and I (data not shown) are similar. ***e***, A fragment of the crystal structure of mineral HfO_2. MolScript[39] was used to generate (*b*–*e*).

The sequential motif Tyr195-Tyr196 is absolutely conserved in all Fbps and is essential for cluster recognition. Iron binding to Fbp is abolished when either Tyr195 or Tyr196 is mutated[25,26]. Although in mammalian transferrins the two Tyr ligands come from distant parts of the sequence (Tyr95 and Tyr188 in the N-lobe, and Tyr426 and Tyr517 in the C-lobe of human transferrin), a dityrosyl motif is nevertheless highly conserved in the N-lobe (Tyr95-Tyr96). Further work is required to elucidate the potential multinuclear binding mode for mammalian transferrins.

Biological implications

Our discovery of oxo-metal clusters bound in the open cleft of a protein that was previously considered to accommodate only a single metal ion suggests the possibility of an alternative iron uptake mechanism. On the basis of available structures of apo and mononuclear holo-forms, the acquisition of metal ions by transferrins is usually thought to involve a series of steps[22]: binding of a synergistic anion in the open cleft, coordination of metal to a tyrosine side chain, loss of ligands from the presenting metal complex and lobe closure to give a mononuclear adduct. Although native Fe–nFbp contains a single metal ion anchored to two tyrosines in a closed inaccessible binding pocket and cannot take up further metal ions, our study of Hf–nFbp has revealed that each tyrosine can bind to a separate metal ion. The tyrosines bring these metal ions into close proximity, stimulating further growth of the cluster. Oxygens from the cluster replace the synergistic anion. Hence, the metal uptake pathway may also include bound multinuclear intermediates. Our findings also illustrate how a flexible protein-binding cleft can play a major role in controlling the growth/dissimilation of nanominerals.

Iron is an essential nutrient, but soluble low–molecular-weight forms of iron are scarce in the environment even though iron oxides are abundant. Polymeric oxide- and hydroxide-bridged species are often the major forms of highly charged metal ions present in aqueous media[6,27]. Intriguingly, bacterial transferrins seem to be capable of sampling the cell surface[28], and the ability to recognize multimetal clusters may allow them to acquire iron from minerals under iron-limiting conditions. It is notable that the dissimilatory metal ion–reducing bacterium *Shewanella oneidensis* MR-1, which can adhere to mineral surfaces, has an Fbp analog (27% identity including conserved Tyr-Tyr motif) and shows closest phylogenetic similarity to pathogenic microbes[29] — a possible indication of the evolutionary origin of cluster-binding ability.

Methods

Protein synthesis and characterization. Wild type nFbp was expressed[30] in TOP10 *E. coli* cells (Invitrogen) containing the plasmid pTrc99A/Fbp/Ng and purified by cation exchange chromatography[31]. The concentration of holo-nFbp was determined from ε_{481} = 2,430 M^{-1} cm^{-1} or ε_{280} = 48,900 M^{-1} cm^{-1} (ref. 30). Total protein was also determined from the S content by ICP-AES (inductively coupled plasma-atomic emission spectrometry) (1 S per mol protein: Met308; Thermo Jarrell Ash IRIS). Fe and phosphate (as well as Ti, Zr and Hf) were also determined by ICP-AES. Values are averages of three determinations on each sample. nFbp contained a ~1:1 mol ratio of bound Fe:P as found[7,9], although phosphate was readily lost during purification in Tris buffer (Table 1). Fe was removed by treatment of holo-nFbp with excess sodium citrate at pH 4.5 in a Centricon-10 microconcentrator (Amicon) or at pH 6 with nFbp bound to a Resource S column (Amersham) followed by elution with 10 mM

Table 2 Crystallographic data and refinement statistics[1]

Parameter	Crystal 1	Crystal 2
Wavelength (Å)	0.87	0.87
Resolution	20.0–1.7 (1.72–1.76)	30.0–1.6 (1.63–1.60)
Refined twinning fraction (%)	19.9	43.8
Completeness (%)[2]	98.2 (52.0)	100.0 (100.0)
I / σ^2	4.4 (1.0)	7.4 (1.8)
R_{sym} (%)[2,3]	6.5 (45.1)	8.0 (58.4)
R_{cryst} (%)[4]	–	16.5
R_{free} (%)[5]	–	26.4
R.m.s. deviations		
Bonds (Å)	–	0.006
Angles (°)	–	1.24
Average *B*-factors		
Protein (Å^2)	–	31.3
Water (Å^2)	–	33.5

[1]The data from the more asymmetric crystal 1 were used to solve the structure, and better data from crystal 2 were used for refinement.
[2]Values in parentheses are for the highest resolution shell.
[3]$R_{sym} = \Sigma|I_h - \langle I_h \rangle| / I_h$, where $\langle I_h \rangle$ is the average intensity over symmetry equivalent reflections.
[4]$R_{cryst} = \Sigma||F_o| - |F_c|| / \Sigma|F_o|$, where summation is over the data used for refinement.
[5]R_{free} was calculated using 7% of data excluded from refinement.

Tris-HCl buffer and a 0–1 M NaCl gradient. Apo nFbp concentrations were determined at ε_{280} = 44,200 M^{-1} cm^{-1} (ref. 30). Metal-loaded and apo proteins were purified by ultrafiltration three times using Centricon YM-30 ultrafilters (Amicon). In some cases, a previous step of passage through a PD-10 (Amersham) column was used as to obtain an initial separation.

Crystallography. Hf–nFbp was prepared by reacting apo nFbp with 4 mol equivalent of $[Hf(NTA)_2]^{2-}$ (using the crystalline mononuclear complex $Na_2[Hf(NTA)_2]\bullet 2H_2O$) for 3 h at 310 K in 100 mM NaCl, 4 mM phosphate and 25 mM $NaHCO_3$, pH 7.4. Small molecules (<30 kDa) were removed by ultrafiltration using 0.1 M KCl. Reaction with either 50 or 100 mol equiv of $[Hf(NTA)_2]^{2-}$ gave similar results. Crystals were grown by the hanging drop technique at 290 K in ~20% (w/v) PEG 4000, 0.2 M KCl and 0.4 M imidazole/malate buffer, pH 7.7. The crystals were flash-frozen in liquid N_2, and the X-ray data were collected on stations 14.1 and 9.6 (SRS, Daresbury Laboratory) using an ADSC Quantum4 CCD detector, and processed and scaled with HKL2000 (ref. 32). Crystals belong to the space group $P3_2$ ($a = b$ = 148.1 Å and c = 115.8 Å) and were ~50% twinned. All except one data set (crystal 1, Table 2) could also be processed in the space group $P3_212$. This crystal 1 was used for structure determination, and a higher resolution data set from crystal 2 (Table 2) was used for final refinement. The structure was solved by a combination of molecular replacement and SAD using CCP4 suite[33] and CNS[34]. Both AMoRe[35] and MOLREP[33] produced the same mutual disposition of six protein molecules that obey two-fold noncrystallographic rotation axes parallel to the twinning axis of the crystal (search model PDB entry 1D9Y). Three remaining molecules were found by manual analysis of the anomalous differences (originating from Hf^{4+}) combined with the phases from the molecular replacement model. Subsequent twinned rigid body refinement using CNS reduced R_{cryst} to 36% and R_{free} to 38%. The positions of all Hf^{4+} ions were confidently revealed by the difference Fourier map generated with coefficients ($F_o - F_c$) and the phases calculated from the final protein model. Anomalous difference Fourier maps confirmed that these peaks of electron density belong to Hf ions (f'' = 9 e$^-$ at a wavelength of 0.87 Å). We performed nine cycles of manual rebuilding with O[36] followed by positional refinement, *B*-factor refinement, twinning fraction refinement and automatic water building with CNS. We used bond angles and lengths from inorganic HfO_2 in the Chemical Database Service (*http://www.cds.dl.ac.uk/cds/*) as the targets for refinement. The final model is the result of crystal 2 refinement (Table 2).

Coordinates. Coordinates have been deposited in the Protein Data Bank (accession code 1O7T).

Acknowledgments
We thank The Wellcome Trust (Edinburgh Protein Interaction Centre, fellowships for D.J.B.H. and W.Z., and International Research Development Award for W.Z.), Darwin Trust (fellowship for D.A.) and CVCP (ORS Awards for H.Z. and M.G.) for their support for this work, and G.G. Dodson, E.I. Stiefel, A.J. Thomson and R.J.P. Williams for their helpful comments on this script.

Competing interests statement
The authors declare that they have no competing financial interests.

Received 4 September, 2002; accepted 6 January, 2003.

1. Pennisi, E. Geobiologists: as diverse as the bugs they study. *Science* **296**, 1058–1060 (2002).
2. Mann, S. Biomineralization: Principles and Concepts in Bioinorganic Materials Chemistry (Oxford University Press, New York; 2001).
3. Newmann, D.K. & Banfield, J.F. Geomicrobiology: how molecular-scale interactions underpin biogeochemical systems. *Science* **296**, 1071–1077 (2002).
4. Butler, A. Acquisition and utilization of transition metal ions by marine organisms. *Science* **281**, 207–210 (1998).
5. Ratledge, C. & Dover, L.G. Iron metabolism in pathogenic bacteria. *Annu. Rev. Microbiol*. **54**, 881–941 (2000).
6. Crichton, R.R. *Inorganic Biochemistry of Iron Metabolism* (Ellis Horwood, New York; 1991).
7. Bruns, C.M. *et al.* Fe^{+3}-binding protein reveals convergent evolution within a superfamily. *Nat. Struct. Biol.* **4**, 919–924 (1997).
8. Bruns, C.M. *et al*. Crystallographic and biochemical analyses of the metal-free *Haemophilus influenzae* Fe^{3+}-binding protein *Biochemistry* **40**, 15631–15637 (2001).
9. Taboy, C.H., Vaughan, K.G., Mietzner, T.A., Aisen, P. & Crumbliss, A.L. Fe^{3+} Coordination and redox properties of a bacterial transferrin. *J. Biol. Chem.* **276**, 2719–2724 (2001).
10. Aisen, P. Iron metabolism: an evolutionary perspective. in *Iron Metabolism in Health and Disease* (eds. Brock, J. H., Halliday, J.W., Pippard, M.J. & Powell, L.W.) 1–30 (W.B. Saunders Co., London; 1994).
11. Sun, H., Cox, M.C., Li, H. & Sadler, P.J. Rationalisation of metal binding to transferrin: prediction of metal-protein stability constants. *Struct. Bonding* **88**, 71–102 (1997).
12. Yang, X.J. & Pin, C. A novel solid-phase extraction scheme for the group separation of high field strength elements (Nb, Ta, Zr, Hf) from Al-, Ti-, and Fe-rich geological materials. *Sep. Sci. Technol*. **36**, 571–585 (2001).
13. Schwietert, C.W. & McCue, J.P. Coordination compounds in medicinal chemistry. *Coord. Chem. Rev.* **184**, 67–89 (1999).
14. Guo, M., Sun, H., McArdle, H.J., Gambling, L. & Sadler, P.J. Ti(IV) uptake and release by human serum transferrin and recognition of Ti(IV)-transferrin by cancer cells: understanding the mechanism of action of the anticancer drug titanocene dichloride. *Biochemistry* **39**, 10023–10033 (2000).
15. Then, G.M., Appel, H., Duffield, J., Taylor, D.M. & Thies, W.-G. *In vivo* and *in vitro* studies of hafnium-binding to rat serum transferrin. *J. Inorg. Biochem.* **27**, 255–270 (1986).
16. Ruh, R. & Corfield, P.W.R. Crystal structure of monoclinic hafnia and comparison with monoclinic zirconia. *J. Am. Ceram. Soc.* **53**, 126–129 (1970).
17. Evans, W.J., Ansari, M.A. & Ziller, J.W. Isolation and structural characterization of the polymetallic zirconium alkoxide complexes, $Zr_3O(OCH_2CMe_3)_9Cl$, $Zr_3O(OCMe_3)_9(OH)$, and $Na_4Zr_6O_2(OEt)_{24}$. *Polyhedron* **17**, 869–877 (1998).
18. Starikova, Z.A. *et al*. Structural study of zirconium and hafnium oxoalkoxides. *Polyhedron* **18**, 941–947 (1999).
19. Schmid, B. *et al*. Structure of a cofactor-deficient nitrogenase MoFe protein. *Science* **296**, 352–356 (2002).
20. Mizutani, K., Yamashita, H., Kurokawa, H., Mikami, B. & Hirose, M. Alternative structural state of transferrin. The crystallographic analysis of iron-loaded but domain-opened ovotransferrin N-lobe. *J. Biol. Chem.* **247**, 10190–10194 (1999).
21. Khan, J.A., Kumar, P., Srinivasan, A. & Singh, T.P. Protein intermediate trapped by the simultaneous crystallization process. Crystal structure of an iron-saturated intermediate in the Fe^{3+} binding pathway of camel lactoferrin at 2.7 Å resolution. *J. Biol. Chem*. **276**, 36817–36823 (2001).
22. Kuser, P. *et al*. The mechanism of iron uptake by transferrins: the X-ray structures of the 18 kDa NII domain fragment of duck ovotransferrin and its nitrilotriacetate complex. *Acta Crystallogr. D* **58**, 777–783 (2002).
23. Grossmann, J.G. *et al*. Metal-induced conformational changes in transferrins. *J. Mol. Biol*. **229**, 585–590 (1993).
24. Jeffrey, P.D. *et al*. Ligand-induced conformational change in transferrins: crystal structure of the open form of the N-terminal half-molecule of human transferrin. *Biochemistry* **37**, 13978–13986 (1998).
25. Nowalk, A.J., Vaughan, K.G., Day, B.W., Tencza, S.B. & Mietzner, T.A. Metal-dependent conformers of the periplasmic ferric ion binding protein. *Biochemistry* **36**, 13054–13059 (1997).
26. Guo, M. Proteins and nucleic acids as targets for titanium(IV). PhD thesis, Univ. Edinburgh (2000).
27. Frausto da Silva, J.J.R. & Williams, R.J.P. The principles of the uptake and chemical speciation of the elements in biology. in *The Biological Chemistry of the Elements.* Chapter 2, 23–70 (Oxford University Press, Oxford; 1991).
28. Ferreiros, C., Criado, M.T. & Gomez, J.A. The Neisserial 37 kDa ferric binding protein (FbpA). *Comp. Biochem. Physiol. Biochem. Mol. Biol.* **123**, 1–7 (1999).
29. Heidelberg, J.F. *et al*. Genome sequence of the dissimilatory metal ion-reducing bacterium *Shewanella oneidensis*. *Nat. Biotechnol.* **20**, 1118–1123 (2002).
30. Guo, M. *et al.* Synergistic anion and metal binding to the ferric-ion binding protein from *Neisseria gonorrheae* (nFBP). *J. Biol. Chem.* **278**, 2490–2502 (2003).
31. Nowalk, A., Tencza, S. & Mietzner, T. Coordination of iron by the ferric iron-binding protein of pathogenic *Neisseria* is homologous to the transferrins. *Biochemistry* **33**, 12769–12775 (1994).
32. Otwinowski, Z. & Minor, W. Processing of X-ray diffraction data collected in oscillation mode. *Methods Enzymol.* **276**, 307–326 (1997).
33. Collaborative Computational Project, Number 4. The CCP4 suite: programs for protein crystallography. *Acta Crystallogr. D* **50**, 760–763 (1994).
34. Brunger, A.T. *et al*. Crystallography & NMR system: a new software suite for macromolecular structure determination. *Acta Crystallogr. D* **54**, 905–921 (1998).
35. Navaza, J. & Saludjian, P. AMoRe: an automated molecular replacement program package. *Methods Enzymol*. **276**, 581–594 (1997).
36. Jones, T.A. & Kjeldgaard, M. *O Version 5.9, The Manual* (Uppsala University, Uppsala; 1994).
37. Nicholls, A., Sharp, K.A. & Honig, B. Protein folding and association: insights from the interfacial and thermodynamic properties of hydrocarbons. *Proteins* **11**, 281–296 (1991).
38. Read, R.J. Improved Fourier coefficients for maps using phases from partial structures with errors. *Acta Crystallogr. A* **42**, 140-149 (1986).
39. Kraulis, P.J. MOLSCRIPT: a program to produce both detailed and schematic plots of protein structures. *J. Appl. Crystallogr.* **24**, 945–949 (1991).
40. Sun, H., Li, H., Weir, R.A. & Sadler, P.J. The first specific Ti(IV)-protein complex: potential relevance to anticancer activity of titanocenes. *Angew. Chem. Int. Ed. Engl.* **37**, 1577–1579 (1998).

A novel protein–mineral interface

Dmitriy Alexeev, Haizhong Zhu, Maolin Guo, Weiqing Zhong, Dominic J.B. Hunter, Weiping Yang, Dominic J. Campopiano and Peter J. Sadler

Nature Structural Biology; doi: 10.1038/nsb903

In the version of this article initially published online, the institution affiliations were assigned incorrectly because of a mistake that occurred during production. The correct affiliations for all authors are as follows: Dmitriy Alexeev[1], Haizhong Zhu[2], Maolin Guo[2,3], Weiqing Zhong[2,4], Dominic J.B. Hunter[2], Weiping Yang[2,3], Dominic J. Campopiano[2] and Peter J. Sadler[2]. All of the footnotes (corrected) are as follows: [1]Institute of Cell and Molecular Biology, Michael Swann Building, University of Edinburgh, Mayfield Road, Edinburgh EH9 3JR, UK; [2]School of Chemistry, University of Edinburgh, West Mains Road, Edinburgh EH9 3JJ, UK; [3]Current address: Department of Molecular Biology and Biochemistry, University of California, Irvine, California 92697, USA; and [4]Current address: School of Pharmacy, Second Military Medicine University, Shanghai 200433, China. We apologize for any inconvenience this may have caused. This mistake has been corrected in the HTML and print version of the article.